



## Design and Evaluation of a Magnetorheological Damper Based Prosthetic Knee

S. Seid<sup>\*a</sup>, S. Chandramohan<sup>b</sup>, S. Sujatha<sup>b</sup>

<sup>a</sup> Production Engineering Department, College of Engineering, Defence University, Bishoftu, Ethiopia

<sup>b</sup> Mechanical Engineering Department, Indian Institute of Technology Madras, Chennai, India

### PAPER INFO

#### Paper history:

Received 12 May 2018

Received in revised form 30 December 2018

Accepted 03 January 2019

#### Keywords:

Knee

Swing Phase

Magnetorheological (MR) Damper

Damping Force

### ABSTRACT

In this work, a magnetorheological (MR) damper based above-knee prosthesis is design and evaluated based on its performance in swing phase and in stance phase. Initially, a dynamic system model for swing phase of a prosthetic leg incorporating a single-axis knee with ideal MR damper was built. The dynamic properties of the damper are represented with Bingham parametric model. From Bingham model, governing damper parameters that determine the damping force and piston displacement of the damper are identified and optimized so as to enable the single-axis knee to nearly mimick the natural swing phase trajectory of a healthy person for level-ground walking as obtained from experimental data. Then, with the optimal damper parameters, an MR damper valve constrained in a desired cylindrical volume is developed. Finally, the prosthetic knee with the MR damper is evaluated for its performance during stance phase, based on ISO standard loading condition for the intended application. The results show that, compare to Rheo knee<sup>®</sup>, the MR damper based prosthetic knee has achieved up to 68% reduction by volume and 40% reduction by weight.

doi: 10.5829/ije.2019.32.01a.19

### NOMENCLATURE

$m_1$ and $m_2$	Masses of thigh and shank	$A_p$ and $A_s$	Piston and shank cross sectional areas
$a_1$ and $a_2$	Distances of the mass centres of thigh and shank from the respective proximal joints	$G$	Complex shear modulus
$I_1$ and $I_2$	Moments of inertia for thigh and shank	$P_a$	Pressure in gas chamber
$l_1$ and $l_2$	Lengths of thigh and shank	$k$	Coefficient of thermal expansion
$s$	Offset between the knee centre and location of damper attachment on the thigh	$x_p$	Displacement of the piston
$l_d$	Length of the damper	$c$	Coefficient of the flow velocity profile
$b$	Distance between the knee centre and location of the damper attachment on the shank	$R_l$	Average radius of the duct
$x_h$	Horizontal movement of the hip	<b>Greek Symbols</b>	
$y_h$	Vertical movement of the hip	$\theta_1$ and $\theta_2$	Absolute angles of thigh and shank from the horizontal
$T_l$	Hip torque	$\theta_t$ and $\theta_s$	Absolute angles of thigh and shank respectively from the vertical
$F_d$	Damping force	$\theta_k$	Knee angle
$F_{MR}$	Frictional force	$\tau$	Fluid shear stress
$C_{vis}$	Damping coefficient	$\tau_y$	Yield stress developed as result of applied field
$F_o$	Offset in the force due to the presence of the accumulator	$\dot{\gamma}$	Fluid shear strain rate
$P_o$	Initial pressure of the gas chamber	$\gamma$	Fluid shear strain
$V_o$	Initial volume of the gas chamber	$\eta$	Plastic viscosity of MR fluid without applied magnetic field

\*Corresponding Author Email: solomonseid@gmail.com (S. Seid)

Please cite this article as: S. Seid, S. Chandramohan, S. Sujatha, Design and Evaluation of a Magnetorheological Damper Based Prosthetic Knee, International Journal of Engineering (IJE), IJE TRANSACTIONS A: Basics Vol. 32, No. 1, (January 2019) 146-152

## 1. INTRODUCTION

Above-knee amputation is one of the most common types of amputation in the world. A person with an above-knee amputation requires a prosthetic leg to stand and walk again. Any prosthetic leg used must be able to restore the functionality of the lost muscles and achieve near normal human gait. There are two phases that characterize human gait, a stance phase and a swing phase. In the stance phase, a foot is in contact with the ground, while in the swing phase, the lower limb swings through following toe-off. These functional necessities of human gait have to be provided by the prosthetic leg. Particularly, the prosthetic knee, which is the most complex part of above-knee prostheses, plays a key role in providing knee stability during stance phase and damping during the swing phase.

Prosthetic knees designed with passive mechanisms such as friction, spring and damping coefficients generally lack active knee joint control and as a result they are not sufficient to mimic natural human walking. Prosthetics equipped with active knee joint control such as hydraulic actuation (C-Leg™ by Otto Bock) are able to produce a gait near to natural one; however, they have limitation in terms of cost, weight, energy consumption and responses when the battery runs out [1, 2]. In this regard, for the last two decades, many researchers have considered a semi-active intelligent driving device, an MR damper, as a driver of the prosthetic knee.

Prosthetic knees incorporating off-the-shelf MR damper such as RD-1005-3, manufactured by Lord Corporation, are reported for their drawbacks [3]. This work proposes an integrated design approach for an MR damper based prosthetic knee where reported drawbacks of such prosthetic knees are addressed. Such design approach has also been suggested in literature [4] and adopted for other applications, also reported in literature [5-7]. Moreover, there have been also efforts to upgrade the performances of the MR damper valves [8], authors' previous work.

Therefore, this work is aimed at disclosing an integrative design approach for an MR damper based prosthetic knee with the objective of addressing the aforementioned drawbacks. First, a single-axis prosthetic knee incorporating the desired MR damper is developed by considering stability aspects and aesthetics. Then, a dynamic system model of the swing phase leg for the normal level-ground walking is adopted, and based on this model and experimental gait data from literature; the damper is designed. Then, the designed damper integrated in the prosthetic knee is evaluated whether to produce required damping force for walking. The overall knee structure should also withstand ISO standard stance phase loading conditions and be light in weight.

## 2. SINGLE-AXIS KNEE WITH AN MR DAMPER

A single-axis prosthetic knee is designed initially by taking into account knee stability during stance phase and aesthetic aspects [9]. Dimensional constraints within which a desired MR damper is to be incorporated are determined. The single-axis knee has one degree of freedom and is to be attached to the socket housing the residual limb of an above-knee amputee (Figures 1(a) and 1(b)). The CAD Model of the knee with desired MR damper is shown in Figure 1(c). The authors, in their previous work [10], have designed an MR damper based single-axis knee by considering the swing-phase where the damping effect is predominant and dynamic properties of the MR damper, Figure 1(d), was also represented by Bingham model [11]. The methodology and dynamic system model, shown in equation of motion were already developed, hence in this work, they are adopted except with the following dimensional input variations: an offset distance for the attachment of the damper from the knee axis,  $s$ , is taken to be 30mm, the damper's fully extended length and stroke are taken to be 129.51mm and 28.13 mm, respectively, outer diameter of the MR damper's main cylinder is 38 mm, and maximum operating input current is limited to be 1 A. With these input variations, the optimal damper parameters are determined to be  $C_{vis} (Ns/m)=27.2319$ ,  $F_{MR}(N)=187.000$ ,  $F_o (N)=-269.661$ . Experimental data of normal hip, thigh and shank motions are adopted from literature [12] for the normal level-ground walking

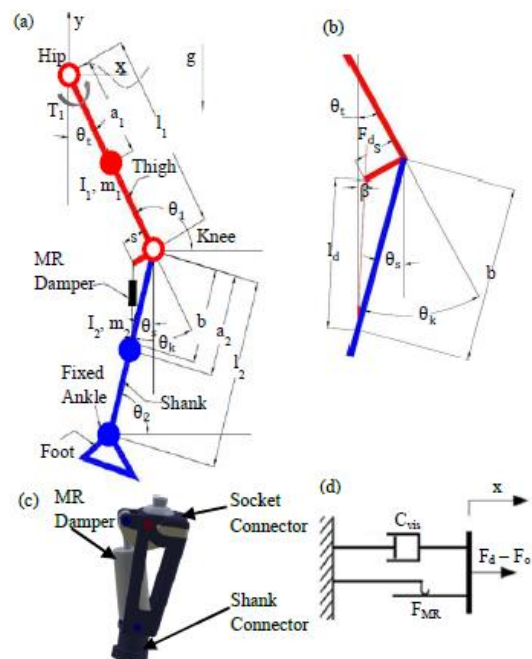


**Figure 1.** (a) The amputee's swing leg model, (b) damper force resolution, (c) CAD model of the knee with desired MR damper and (d) Bingham model of a controllable damper

of a person with 56.7 kg body mass at an average velocity of 1.3 m/s from toe-off to heel-strike. Physical parameters of the model are computed based on anthropometric table [12] for the person and are listed as:  $M=56.7$  kg,  $l_1=0.314$  m,  $l_2=0.425$  m,  $m_1=5.67$  kg,  $a_1=0.136$  m,  $m_2=3.46$  kg,  $a_2=0.2576$  m,  $I_1=0.058$  kgm<sup>2</sup>,  $I_2=0.108$  kgm<sup>2</sup>. Evaluation of swing phase with respect to normal is depicted in Table 1, and results are acceptable to clear the ground in level-ground walking with the prosthetic knee.

Simplified form of equation of motion:

$$L\ddot{\theta}_s = F_d M \sin(\theta_s - \beta) + N \cos \theta_s + P \sin \theta_s \quad (1)$$

where,  $L = -(m_2 a_2^2 + I_2 / m_2 a_2)$ ,

$$N = -l_1 \cos \theta_t \ddot{\theta}_t + l_1 \sin \theta_t (\dot{\theta}_t)^2 - \ddot{x}_h,$$

$$P = l_1 \sin \theta_t \ddot{\theta}_t + l_1 \cos \theta_t (\dot{\theta}_t)^2 + g - \ddot{y}_h, \quad M = b / m_2 a_2$$

$$\text{and } \beta = \cos^{-1} \left( \frac{1 - \frac{b}{s} \sin \theta_k}{\sqrt{1 + \frac{b}{s} - 2 \frac{b}{s} \sin \theta_k}} \right) - \theta_t - 90^\circ.$$

According to Bingham's MR damper model, the damping force,  $F_d$ , for non-zero piston velocities,  $\dot{x}$ , is given by Nguyen and Choi [5]:

$$F_d = F_{MR} \operatorname{sgn}(\dot{x}) + C_{vis} \dot{x} + F_o \quad (2)$$

where:

$$F_{MR} = (A_p - A_s) \frac{2cL_p}{g_l} \tau_y, \quad C_{vis} = \frac{6\eta H}{\pi R_l g_l^3} (A_p - A_s), \quad F_o = P_o A_s,$$

$P_o = P_o \left( \frac{V_o}{V_o + A_s x_p} \right)^k$ ,  $c = 2.07 + \frac{12Q\eta}{12Q\eta + 0.8\pi R_l d^2 \tau_y}$  and  $R_l = R - d - 0.5g_l$ . The parameter  $k$  varies between 1.4 and 1.7. The parameter  $c$  has a value varying from 2.07 to 3.07.

Maximum required damping force during stance phase and swing phase is computed using the optimal damper parameters and the experimental data of normal level-ground walking, and it is found to be about 459.65 N, Figure 2. Hence, the ideal MR damper is expected to produce at least this amount of damping force. From Figure 2, one can also see that the damping force is higher from toe-off up to 0.266 seconds and again from 0.336 seconds until the end of swing phase; this is expected because of the fact that a higher damping force is required in most of the swing phase as the shank is extending and again near the end of the swing phase to dampen the impact load which is produced as a result of foot contact with the ground. On the other hand, the damping force remains lower in most of stance phase region as most of the weight bearing is taken care of by the prosthetic knee structure, but becomes higher from 0.858 seconds to the end of stance phase, which is also expected as the shank undergoes flexion near the end of the stance phase where the knee is bending to initiate the swing phase.

**TABLE 1.** Evaluation of swing phase with respect to normal

Simulation	Maximum knee angle (degree)	Shank velocity at 0.3 s (rad/s)	Root-mean-square error (degree)
Normal	60.563	3.885	-
MR Damper	50.200	4.363	6.113

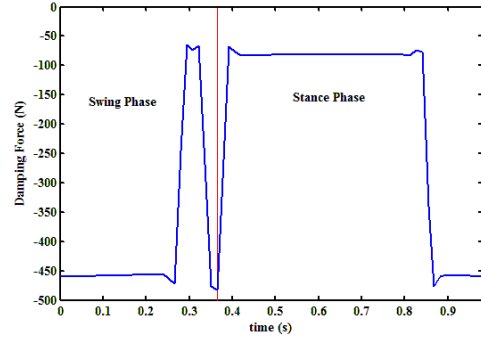


**Figure 2.** Damping force versus time for swing phase and stance phase at 1 Ampere

### 3. DESIGN OF AN MR DAMPER VALVE

The MR damper valves consist of a piston over which the coil is wound and a gap is maintained between the inner and outer pistons. The piston is made up of low carbon cold rolled steel SAE 1020 due to its high relative permeability. Materials adopted for an MR damper valve are: SAE1020 for valve core and valve housing, Copper (24-gauge) for coil, and MRF132-DG for the MR fluid. Relative permeability is determined by B-H curve of respective materials. Schematic configuration of a single-coil MR damper and valve with annular duct are shown in Figure 3. Based on the aforementioned geometrical constraints imposed on the prosthetic knee and the MR damper, parameters of MR damper valve, which are to be used in the computation of MR damping force, were optimally designed for the intended application in author's previous work [13], and are listed as: Active Pole Length,  $L_p=8$  mm; Coil Width,  $W_c=4.4914$  mm; Outer Piston Thickness,  $d=3$  mm; Duct Gap Length,  $g_l=0.9127$  mm; Radius of the Valve,  $R=16$  mm; Height of the Valve,  $H=20$  mm; Copper Wire Diameter (for 24-gauge),  $d_c=0.51$  mm; Initial Pressure of the Gas Chamber,  $P_o=5.45$  N/mm<sup>2</sup>, Initial Volume of the Gas Chamber,  $V_o=6371.15$  mm<sup>3</sup>, Displacement of the Piston,  $x_p=28.13$  mm; Radius of Piston Shaft,  $R_s=5$  mm, Range of Applied Current,  $I=0.1-1$  A; and Number of Turn of Coil,  $N=294$ . For the purpose of finite element analysis, 2-D axi-symmetric MR damper valve, shown in Figure 4(a) is considered. Considering the valve geometric dimensions, number of elements per line is used for specifying meshing size.

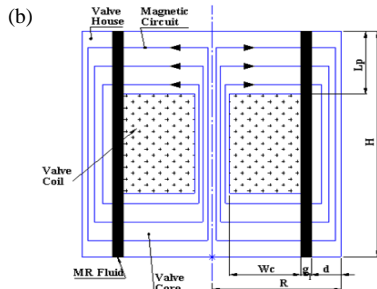
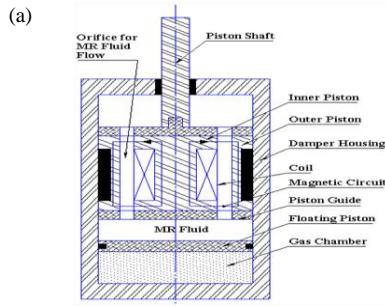


**Figure 3.** Schematic configuration of a single-coil MR damper and valve. (a) MR damper, (b) MR valve

Several simulations with different mesh size have been conducted in order to find optimum mesh size, which generates accurate results efficiently. The number of elements on the lines across the MR fluid orifice is specified as a parameter called a basic meshing number. The number of elements of other lines in the model is selected as a product of the basic meshing number and an appropriate scalar. This method of meshing has also been adopted in previous work [5]. For this work, it has been found that the basic meshing number 23 is sufficiently accurate to ensure the convergence of the finite element solution. The 2D axi-symmetric finite element model of the adopted configuration of the damper valve is also shown in Figure 4(b). The model is analyzed and computed for the variation of magnetic field intensity and magnetic flux density along the active length of the pole (Figure 4(c)), in ANSYS 2014, with PLANE53 elements; they are computed as follows [5]:

$$B_{MR} = \int_0^{L_p} B_{MR}(s) ds / L_p \quad (3)$$

$$H_{MR} = \int_0^{L_p} H_{MR}(s) ds / L_p \quad (4)$$

In Equations (3) and (4),  $B_{MR}(s)$  and  $H_{MR}(s)$  are the magnetic flux density and magnetic field intensity, respectively at each nodal point located on the defined path, AA (Figure 4(c)). The variation of magnetic flux density at 1 Ampere is shown in Figure 5.

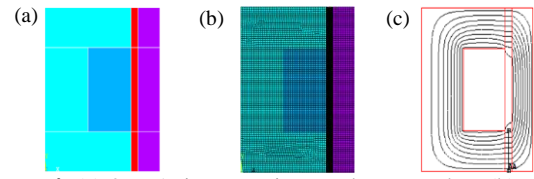


**Figure 4.** (a) 2-D Axisymmetric MR damper valve, (b) Finite element model of the valve and (c) Flux lines around the electrical coil of Model 1 and the path for computing  $H_{MR}$  and  $B_{MR}$ .

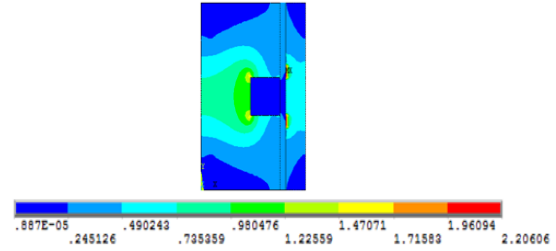


**Figure 5.** Magnetic flux density (Tesla) ( $A/m$ ) of the Optimized MR damper valve at 1 Ampere

In designing an MR damper valve, high damping force due to yield stress is desired, generally. MR damper force is evaluated based on the quasi-static model of MR valves, where the equation is derived based on the assumption that the MR fluid exhibits Bingham plastic behavior and the flow is fully developed in the ducts [14]. Materials adopted for an MR damper valve: SAE1020 for valve core and valve housing, Copper (24-gauge) for coil, and MRF132-DG for the MR fluid. Relative permeability is determined by B-H curve of respective materials. The Bingham's Plastic flow model is given by following equation [14]:

$$\tau = \eta \dot{\gamma} + \tau_y (H_{MR}) \text{sgn}(\dot{\gamma}), |\tau| \geq \tau_y \quad (5)$$

$$\tau = G\gamma, |\tau| < \tau_y$$

Equation (5) is used to design a device which works on the basis of MR fluid. Upon fitting a polynomial to the MR fluid (MRF132-DG) data from Lord Corporation, the induced yield stress of the MR fluid as a function of the applied magnetic field intensity of MR fluid along the pole length,  $H_{MR}$ , can be approximately expressed as follows [5]:

$$\tau_y = C_0 + C_1 H_{MR} + C_2 H_{MR}^2 + C_3 H_{MR}^3 \quad (6)$$

In Equation (6), the unit of the yield stress is in  $kPa$  while that of the magnetic field intensity is in  $kA/m$ . The coefficients  $C_0$ ,  $C_1$ ,  $C_2$ , and  $C_3$ , determined from experimental results by applying the least squares curve fitting method [15], are respectively identified as 0.3, 0.42, -0.00116 and  $1.05 \times 10^{-6}$ . The simulation results depicted in Figure 6 shows variations of the damping force that can be produced by the designed MR damper

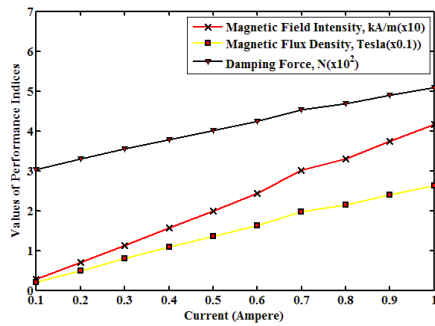


Figure 6. MR damper performance indices

model within the range of 0.1 to 1.0 A. From the simulation result, the designed MR damper valve is capable of producing 589.16 N damping force at 1A, larger than what is required for level-ground walking (459.65 N). Moreover, as the applied current is increased, a wider range of force can be generated by the MR damper as long as  $B_{MR}$  is below the saturation level of the MR fluid. With 3.5 A applied current, which is maximum current carrying capacity of the copper wire (24 gauge), the proposed model can produce up to 698.55 N damping force. Hence it can be concluded that the designed damper is able to produce the required damping force for level-ground walking.

**3. 1. Input Current Variation Effect** Performance test of the designed damper is further conducted through simulation for a sinusoidal excitation of the form in Equation (7). Amplitude and frequency are varying within the range that the prosthetic knee is expected to function for level-ground walking. Sinusoidal excitation displacement is taken to be:

$$x(t) = A_m \sin(2\pi f_r t) \tag{7}$$

where  $A_m$  is the amplitude and  $f_r$  is the frequency of the excitation. The damping force and the input current have a direct relationship. The input current has a significant effect on variations in the amount of damping force. As the input current increases, the damping force will also increase, however it should be noted that when the saturation limit of the MR fluid is reached, any increase in input current cannot increase the damping force. Figure 7 shows the effects of input current on damping force for designed damper. As mentioned earlier, an increase in the input current may cause saturation. For the copper coil adopted in this work, AWG 24, the maximum applied current is 3.5A. To determine whether the MR fluid can saturate, the input current is varied in the range of 0A to 3.5A with an increment of 0.5 for each of the proposed models. The results are shown in Figure 7. It can be observed that within the range of 3A-3.5A input current, as shown in Figure 7, as the current is increasing, the variation in successive damping force is reducing and ultimately

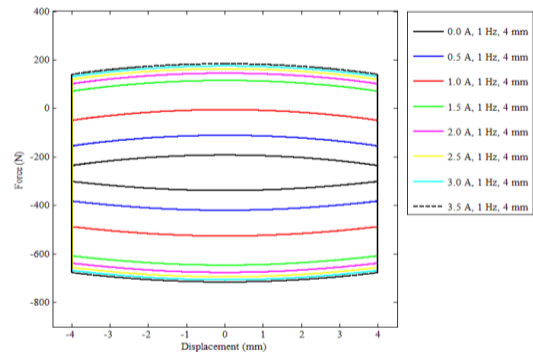


Figure 7. Input current variation effect for MR damper

reaches to the level that damping force does not change (magenta curve and black broken curves), showing that the magnetic valve is heading to saturation.

**4. FEA OF PROSTHETIC KNEE BASED ON ISO**

The prosthetic knee assembly incorporating the MR damper is entirely modelled and finite element analysis (FEA) is performed to investigate the stress characteristics of the prosthetic knee incorporating the designed MR dampers under static loading conditions for real human data based on ISO 10328:2006 E [16]. It should be noted that the original MR damper based prosthetic knee model complexity was simplified to a simpler model consists of three major parts as indicated in Figure 1(c), namely socket connector, MR damper and shank connector. Minor components are grouped together as bonded surface contact into these three major parts and the major parts are connected with each other at the respective joints as free cylindrical surfaces contacts throughout the FEA analysis. For this purpose, apart from the valve parts and the MR fluid whose materials are mentioned before, materials for other parts of the damper and prosthetic knee are also selected by considering their magnetic properties, structural properties and thermal properties. Materials adopted for the prosthetic knee parts are listed as: stainless steel (SS-304) for spherical pyramid, connecting pins and screws, aluminum alloy (Al7075-T6) for socket connector and shank connector, Nylon-6 for patella. Materials adopted for the MR damper parts are listed as: Al 7075 T6 for the cylinder, top and bottom cylinder caps, top and bottom handles, floating piston guides, shaft and screws, Polytetrafluoroethylene (PTFE) for O-rings and rod wiper, ceramic-coated-steel-304 for bushing, and Teflon for wear strip. For finite element analysis, for consecutive runs of the model, percentage change in von-Mises stress less than 0.5 % is generally considered as converged meshing. Subsequently, the knee assembly model with approximately 823613 nodes and 447333 elements is adopted throughout the

simulation. ISO (ISO 10328:2006 E) [16] specifies two loading conditions: Test loading condition I (Figure 8(a)) is related to the instant of maximum loading occurring early in the stance phase of walking, heel contact, and Test loading condition II (Figure 8(c)) is related to the instant of maximum loading occurring late in the stance phase of walking, push off. In both static loading conditions the maximum von-Mises stress of  $177.43 \text{ MPa}$  (Figure 8(b)) and  $124.32 \text{ MPa}$  (Figure 8(d)) are experienced by accumulator end of cylinder cap and shank connector, respectively. These parts of the knee are made of Al 7075-T6. The yield strength of Al 7075-T6 is  $505 \text{ MPa}$ . The maximum equivalent stresses developed in both the loading conditions are below the yield stress, hence it can be concluded that the design is safe for static loading conditions.

## 5. DISCUSSION

In this work, the design parameters of the damper valve are computed at  $1 \text{ A}$  of current. Therefore, based on the optimally determined damping force information which is extracted from the swing phase of normal level-ground walking through optimization, damper valve is enabled to produce the required damping force needed for level-ground walking and achieves a wider range of variable force. For microprocessor controlled knee application, it is generally desirable to have a wider range of force so as to enable the user to walk on different terrains and walking conditions. Based on the wire gauge's current carrying capacity, a wider range of force can also be generated as long as  $B_{MR}$  is below the MR fluid material saturation level.

Apart from the valve parts and the MR fluid whose materials are mentioned before, materials for other parts of the damper are also selected by considering their magnetic properties, structural properties and thermal properties. The materials adopted are Al 7075 T6 for the cylinder, top and bottom cylinder caps, top and bottom handles, floating piston guides, shaft and screws, Polytetrafluoroethylene (PTFE) for O-rings and rod wiper, ceramic-coated-steel-304 for bushing, and Teflon for wear strip. Hence, from the CAD model and the materials adopted, weight of the designed MR damper is computed to be about  $281 \text{ grams}$ , which is significantly lower than commercially available MR dampers for prosthetic knee application, such as MR damper manufactured by Lord Corporation (MR-8040-1), which weighs  $980 \text{ grams}$ . Moreover, considering Rheo knee<sup>®</sup>, which is commercially well known MR damper based single-axis prosthetic knee, has  $686067.2 \text{ mm}^3$  volume and weighs  $1.52 \text{ kg}$  [1]; however, the ideal knee still needs to be more compacted in volume and lighter in weight. Comparing to Rheo knee<sup>®</sup>, the designed MR damper based prosthetic knee is found to have  $219541.5$

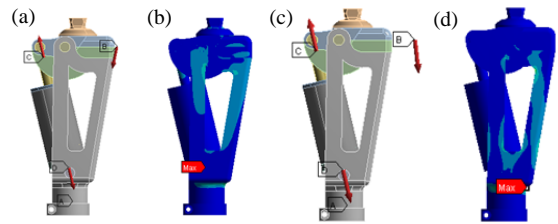


**Figure 8.** a) Static loading condition I, b) Von-Mises stress distribution with loading condition I, c) Static loading condition II, d) Von-Mises stress distribution with loading condition II

$\text{mm}^3$  volume (68% reduction by volume) and weighs about  $0.916 \text{ kg}$  (40% reduction by weight). Furthermore, corresponding leg mass of a normal person is about  $2.63 \text{ kg}$ , hence the designed MR damper based prosthetic knee provides leeway for approximately one and half kilogram of additional weight to accommodate the tibial extension and additional foot peripherals.

## 6. CONCLUSIONS

In this work, design and evaluation of an MR damper based prosthetic knee is presented. Mainly, the swing phase trajectory of normal level ground walking, where damping effect is predominantly required, was considered and experimental data was also introduced into a dynamic system model. Three governing damper parameters were identified and optimized for the intended purpose; subsequently, required optimal damping force for the walking was determined. The MR damper, constrained in a specific volume of a single-axis prosthetic knee, was constructed through FEM tools with the objective of producing the required optimal damping force needed in the swing phase at  $1 \text{ Ampere}$ . Overall, design of an MR damper based prosthetic knee was displayed. The proposed prosthetic knee model is found to be more compacted and lighter than commercially available prosthetic, Rheo knee<sup>®</sup>. The knee assembly has also been proven to withstand ISO standard loading conditions. Future work includes prototyping and conducting dynamic characterization tests of the damper. Knee clinical trials and gait analysis will also be conducted.

## 7. REFERENCES

1. Gudmundsson, K.H., Jonsdottir, F., and Thorsteinsson, F., "A geometrical optimization of a magneto-rheological rotary brake in a prosthetic knee", *Smart Materials and Structures*, Vol. 19, No. 3, (2010), 035023–035033.
2. Seid, S., Sujatha, S., and Chandramohan, S., "Design of controller for single axis knee using hydraulic damper", In IEEE

- AFRICON 2015 Conference , IEEE, (2015), 1–5.
3. Akdogan, K.E., Yilmaz, A., Sadeghimorad, A., and Sahin, I., "Design of semi active knee joint with magnetorheological (MR) damper", In 20th Signal Processing and Communications Applications Conference (SIU), IEEE, (2012), 1–4.
  4. Zhu, X., Jing, X., and Cheng, L., "Magnetorheological fluid dampers: A review on structure design and analysis", *Journal of Intelligent Material Systems and Structures*, Vol. 23, No. 8, (2012), 839–873.
  5. Nguyen, Q.-H., and Choi, S.-B., "Optimal Design Methodology of Magnetorheological Fluid Based Mechanisms", In Smart Actuation and Sensing Systems - Recent Advances and Future Challenges, InTech, (2012).
  6. Djavareshkian, M.H., Esmaceli, A., and Safarzadeh, H., "Optimal Design of Magnetorheological Fluid Damper Based on Response Surface Method", *International Journal of Engineering - Transactions C: Aspects*, Vol. 28, No. 9, (2015), 1359–1367.
  7. Amiri, A., Saeedi, N., Fakhari, M., and Shabani, R., "Size-dependent Vibration and Instability of Magneto-electro-elastic Nano-scale Pipes Containing an Internal Flow with Slip Boundary Condition", *International Journal of Engineering - Transactions A: Basics*, Vol. 29, No. 7, (2016), 995–1004.
  8. Seid, S., Sujatha, S., and Chandramohan, S., "Performance Evaluation of Magnetorheological Damper Valve Configurations Using Finite Element Method", *International Journal of Engineering - Transactions B: Applications*, Vol. 30, No. 2, (2017), 303–310.
  9. Radcliffe, C.W., "The Knud Jansen Lecture: Above-knee prosthetics", *Prosthetics and Orthotics International*, Vol. 1, No. 3, (1977), 146–160.
  10. Seid, S., Sujatha, S., and Chandramohan, S., Design and Evaluation of Swing Phase Controllers for Single-axis Knee, ", *International Journal Bioautomation*, Vol. 20, No. 3, (2016), 373-388.
  11. Spencer, B.F., Dyke, S.J., Sain, M.K., and Carlson, J.D., "Phenomenological Model for Magnetorheological Dampers", *Journal of Engineering Mechanics*, Vol. 123, No. 3, (1997), 230–238.
  12. Winter, D.A., The biomechanics and motor control of human gait: normal, elderly and pathological, (4th Edition), Wiley, (2005).
  13. Seid, S., Chandramohan, S., and Sujatha, S., "Optimal design of an MR damper valve for prosthetic knee application", *Journal of Mechanical Science and Technology*, Vol. 32, No. 6, (2018), 2959–2965.
  14. Jolly, M.R., Bender, J.W., and Carlson, J.D., "Properties and applications of commercial magnetorheological fluids", In 5th Annual International Symposium on Smart Structures and Materials, International Society for Optics and Photonics, (1998), 262–275.
  15. Nguyen, Q.H., Nguyen, N.D., and Choi, S.B., "Optimal design and performance evaluation of a flow-mode MR damper for front-loaded washing machines", *Asia Pacific Journal on Computational Engineering*, Vol. 1, No. 3, (2014), 1–14.
  16. ISO 10328:2006 E, "International Standard: Technical Report", ISO, (2006).

## Design and Evaluation of a Magnetorheological Damper Based Prosthetic Knee

S. Seid<sup>a</sup>, S. Chandramohan<sup>b</sup>, S. Sujatha<sup>b</sup>

<sup>a</sup> Production Engineering Department, College of Engineering, Defence University, Bishoftu, Ethiopia

<sup>b</sup> Mechanical Engineering Department, Indian Institute of Technology Madras, Chennai, India

### P A P E R I N F O

چکیده

#### Paper history:

Received 12 May 2018

Received in revised form 30 December 2018

Accepted 03 January 2019

#### Keywords:

Knee

Swing Phase

Magnetorheological (MR) Damper

Damping Force

در این پژوهش، یک دریچه دمپر مگنتورهلولوژیکی (MR) که بر اساس پروتز فوقانی زانو ساخته شده است، بر اساس عملکرد آن در فاز چرخشی و در مرحله ایستایی طراحی و ارزیابی می‌شود. در ابتدا یک مدل پویا سیستم برای فاز نوسان یک پایه پروتز شامل یک زاویه تک محوری با دمپر ایده آل MR ساخته شد. خواص پویای دمپر با مدل پارامتر Bingham نمایان می‌شود. از مدل Bingham، پارامترهای دمپر حاکم بر نیروی محرک و جابجایی پیستون دمپر شناسایی شده و بهینه شده‌اند تا زانوی تک محور را به تقریباً تقلید مسیر طبیعی فیزیکی یک فرد سالم برای پیاده‌روی سطح-زمین از داده‌های تجربی به دست آورند. سپس، با پارامترهای دمپر مطلوب، دریچه دمپر MR محدود شده در حجم استوانه‌ای مورد نظر توسعه یافته است. در نهایت، زانو پروتز با دمپر MR برای عملکرد آن در فاز ایستای، بر اساس شرایط بارگذاری استاندارد ISO برای برنامه مورد نظر ارزیابی می‌شود. نتایج نشان می‌دهد که در مقایسه با زانو Rheo<sup>®</sup>، زانوی پروتز مبتنی بر دمپر MR تا ۶۸٪ کاهش حجم و کاهش وزن ۴۰٪ کاهش یافته است.

doi: 10.5829/ije.2019.32.01a.19